Isolation and Thermal Reactions of the Intermediates from $BrCH_2CH_2OH$ Decomposition on Cu(100) and Oxygen-Precovered Cu(100)

Pei-Teng Chang, Jain-Jung Shih, Kuan-Hung Kuo, Chia-Yuan Chen, Tao-Wei Fu, Dong-Lin Shieh, Yung-Hsuan Liao, and Jong-Liang Lin*

Department of Chemistry, National Cheng Kung University, Tainan, Taiwan, Republic of China

Received: May 14, 2004; In Final Form: May 18, 2004

The reactions of $BrCH_2CH_2OH$ were investigated on clean and oxygen-precovered Cu(100) surfaces under ultrahigh vacuum conditions. Reflection−absorption infrared spectroscopy (RAIRS) studies were performed to examine the surface intermediates that were generated from $BrCH_2CH_2OH$ decomposition. Density functional theory calculations were employed to predict the infrared spectra, assisting in the identification of the reaction intermediates. On Cu(100), $-CH_2CH_2O-$, formed from the simultaneous scission of the bromine−carbon and oxygen−hydrogen bonds of $BrCH_2CH_2OH$ at ∼190 K, decomposed and evolved into C_2H_4 between 210 and 310 K in temperature-programmed reaction/desorption (TPR/D) experiments. A small amount of CH_3CHO desorption was also observed. On oxygen-precovered Cu(100), $-CH_2CH_2O-$ was also generated at lower exposures (<1.5 L) but at the $BrCH_2CH_2OH$ dosing temperature of 115 K. The TPR/D study showed that C_2H_4 with minor amounts of CH_3CHO evolved between 210 and 310 K. However, at higher $BrCH_2CH_2OH$ exposures (≥1.5 L), $BrCH_2CH_2O-$ was the major intermediate formed at ∼200 K. The formation temperature of C_2H_4 and CH_3CHO was extended to ∼400 K in this case.

Introduction

In the study of thermal reactions of ethyl bromide (C_2H_5Br) on Cu(100) at submonolayer coverages, it has been shown that the C−Br bond dissociates at ∼170 K, generating adsorbed ethyl groups. The ethyl groups are stable up to 245 K, at which they undergo β-hydride elimination to form ethylene.[1] In the case of ethanol (C_2H_5OH) on Cu(100) at a monolayer coverage, only a small fraction decomposes to form ethoxide on the surface.[2,3] However, on oxygen-precovered Cu(100), ethanol readily decomposes between 200 and 300 K to form adsorbed ethoxide, which further reacts at ∼350 K to form acetaldehyde.[4,5] 2-Bromoethanol ($BrCH_2CH_2OH$) molecules that were investigated in the present study possess both of the reactive functional groups of C−OH and C−Br. Therefore, compared to the cases of C_2H_5Br and C_2H_5OH, there are several intriguing points in the thermal decomposition of $BrCH_2CH_2OH$ on Cu(100) and oxygen-precovered Cu(100) (O/Cu(100)), including (1) the dissociation kinetics of the C−Br and O−H bonds, which may be coverage-dependent, (2) the types of surface intermediates generated, which are dependent on the C−Br and O−H bond dissociation temperatures, (3) product distribution, and (4) the effect of the oxygen-precovered surface. With respect to the second point, various surface intermediates are possibly generated from $BrCH_2CH_2OH$ decomposition on Cu(100) and on O/Cu(100), such as $BrCH_2CH_2O-$, $HOCH_2CH_2-$, $-CH_2CH_2O-$, $HOCH_2CH_2O-$, and $-OCH_2CH_2O-$. Studies of oxygen-containing compounds on metal surfaces are important for understanding the partial and selective oxidation of hydrocarbons and the deoxygenation of alcohols. Surface intermediates of $BrCH_2CH_2-$ and $-CH_2CH_2-$ are unlikely to be generated from $BrCH_2CH_2OH$ decomposition on the copper surfaces because the C−O breakage pathway has never been observed for alcohol decomposition on Cu or O/Cu.

In the present research, temperature-programmed reaction/desorption (TPR/D) and reflection−absorption infrared spectroscopy (RAIRS) were employed to investigate the adsorption and decomposition of $BrCH_2CH_2OH$ on clean and oxidized Cu(100) surfaces. To compare the experimental results of RAIRS and to assist the infrared analysis, a program based on the density functional theory was implemented to predict the infrared spectra for the surface intermediates of $-CH_2CH_2O-$ and $BrCH_2CH_2O-$ from $BrCH_2CH_2OH$ decomposition.

Experimental Section

All of the experiments were performed in an ultrahigh vacuum (UHV) apparatus, equipped with an ion gun for sputtering, a differentially pumped mass spectrometer for TPR/D, four-grid spherical retarding field optics for low-energy electron diffraction (LEED) and Auger electron spectroscopy (AES), and a Fourier transform infrared spectrometer for RAIRS. The chamber was evacuated by a turbomolecular pump and an ion pump to a base pressure of approximately 3×10^{-10} Torr. The quadrupole mass spectrometer used for the TPR/D study was capable of detecting ions in a 1−500 amu range and of being multiplexed to acquire up to 15 different masses simultaneously in a single desorption experiment. In the TPR/D experiments, the Cu(100) surface was positioned ∼1 mm from an aperture, 3 mm in diameter, leading to the mass spectrometer, and a heating rate of 2 K•s was used. In the RAIRS study, the IR beam was taken from a Bomem FTIR spectrometer and focused at a grazing incidence angle of 85° through a KBr window onto the Cu(100) in the UHV chamber. The reflected beam was then passed through a second KBr window and refocused on a mercury−cadmium telluride (MCT) detector. The entire beam path was purged with a Balston air scrubber for carbon dioxide and water removal. All of the IR spectra were taken at a temperature of about 115 K, with 800−1500 scans and a 4 cm^{-1} resolution. The presented spectra have been ratioed against the

* jonglin@mail.ncku.edu.tw.

10.1021/jp047938p CCC: $27.50
Published on Web 08/06/2004

spectra of a clean Cu(100) surface recorded immediately before the 2-bromoethanol dosing. The Cu(100) single crystal (1 cm in diameter) was mounted onto a resistive heating element and could be cooled to 110 K (with liquid nitrogen) and heated to 1100 K. The surface temperature was measured by a chromel−alumel thermocouple that was inserted into a hole on the edge of the crystal. Cleaning of the surface by cycles of Ar^+ ion sputtering and annealing was done prior to each experiment until no impurities were detected by Auger electron spectroscopy. 2-Bromoethanol (95%) was purchased from Lancaster and subjected to several cycles of freeze−pump−thaw. Oxygen (99.998%) was obtained from Matheson. The purity of $BrCH_2CH_2OH$ was checked by mass spectrometry. The gas manifold for 2-bromoethanol was conditioned by backfilling with saturated 2-bromoethanol vapor pressure overnight. Prior to 2-bromoethanol being added to the chamber, the gas manifold and 2-bromoethanol itself (in a liquid state) were pumped for a while.

The oxidized Cu(100) surface was prepared by exposing a clean Cu(100) surface at 500 K to 30 L (1 L = 1 langmuir = 10^{-6} Torr·s) of O_2, similar to the preparation for the oxidized Cu(100) used in Sexton's study of alcohol.[4] Atomic oxygen was present on the surface after the O_2 treatment, as verified by Auger electron spectroscopy and electron energy loss spectroscopy. It was estimated that the oxygen coverage (θ_o) for the oxidized Cu(100) used in this study was ~0.2 monolayer (ML).[6] The previous study showed that a long-range order started to develop at $\theta_o = 0.34$ ML, and a $(\sqrt{2} \times 2\sqrt{2})$R45° structure was formed at a saturation coverage of $\theta_o = 0.48$ ML.[6]

In our calculations for the infrared spectra of $-CH_2CH_2O-$ and $BrCH_2CH_2O-$, the optimized structures of $-CH_2CH_2O-$ bonded to two Cu atoms and $BrCH_2CH_2O-$ bonded to Cu clusters were obtained by running a Cerius^2-Minimizer module. Universal 1.02 force field[7] was used, and the Cu atoms were considered fixed at their lattice positions. Infrared absorption frequencies and the related molecular vibrations for these optimized structures were then predicted by running a Cerius^2-DMol^3 module,[8] based on the density functional theory,[9] in which double numerical quality basis sets with polarizations, except 2p for hydrogen, and the Perdew−Wang functional for exchange and correlation were used. The double numerical quality basis sets with polarizations were comparable to 6-31G** sets. However, the numerical basis set was much more accurate than a Gaussian basis set of the same size. The calculations were spin-unrestricted and did not include relativistic effects for the core electrons. The infrared spectra of the species were obtained by two-point frequency calculations.

Results and Discussion

$BrCH_2CH_2OH$ Molecular Desorption from Cu(100) and O/Cu(100). Figure 1 shows the temperature-programmed desorption spectra for the indicated exposures of $BrCH_2CH_2OH$ on Cu(100), collected for 31 amu (CH_3O^+) to represent $BrCH_2CH_2OH$ desorption at ~190 K. At an exposure ≥2.5 L, $BrCH_2CH_2OH$ desorbs and grows with exposure. Therefore, a 2.5 L is considered a monolayer coverage. Figure 2 shows the TPD spectra of $BrCH_2CH_2OH$ molecular desorption for the indicated exposures on O/Cu(100). No $BrCH_2CH_2OH$ desorption is observed below 2 L. From 2 to 4 L, $BrCH_2CH_2OH$ mainly desorbs between 150 and 250 K. For an exposure higher than 4 L, additional desorption peaks between 182 and 188 K. The results of $BrCH_2CH_2OH$ desorption are shown first because they help to explain the RAIRS results presented below.

Infrared Absorptions at Multilayer Coverages of $BrCH_2CH_2OH$ on Cu(100). Figure 3 shows the temperature-dependent IR spectra of a Cu(100) surface after dosing 15 L of $BrCH_2CH_2OH$ at 115 K. As shown in Figure 1, an exposure of 15 L renders a coverage of ~6 ML. In the 170 K spectrum, the infrared bands appear at 835, 929, 1006, 1031, 1051, 1084, 1150, 1218, 1280, 1335, 1377, 1426, and 1459 cm^{-1}. Infrared absorptions of CH_x vibrations between 2700 and 3100 cm^{-1} are not shown because the S/N ratios are poor, probably due to very weak absorptions. Similar spectra were measured at 115 and 150 K. Table 1 compares the frequencies of the infrared bands that were observed in the 170 K spectrum of Figure 3 to those of $BrCH_2CH_2OH$ in liquid and vapor states and shows their similar absorptions.[10] The bands in the 170 K spectrum are attributed to adsorbed $BrCH_2CH_2OH$. When the surface was heated to 180 K, all of the $BrCH_2CH_2OH$ bands decreased in

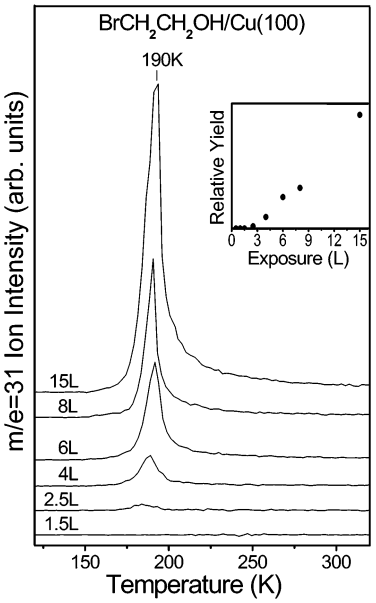

Figure 1. Temperature-programmed desorption spectra for the indicated $BrCH_2CH_2OH$ exposures on a clean Cu(100) surface, collected for 31 amu (CH_3O^+) to represent $BrCH_2CH_2OH$ desorption. The inset shows the relative yield of $BrCH_2CH_2OH$ as a function of the exposure.

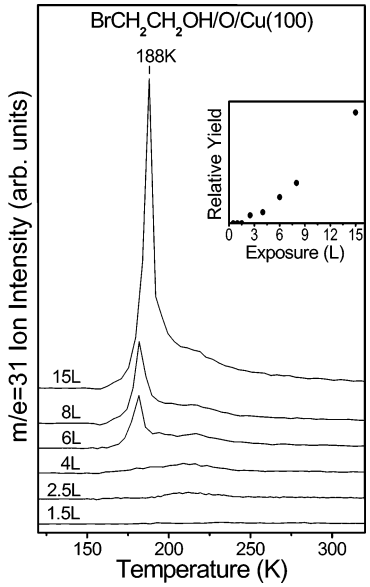

Figure 2. Temperature-programmed desorption spectra for the indicated $BrCH_2CH_2OH$ exposures on an oxygen-precovered Cu(100) surface, collected for 31 amu (CH_3O^+) to represent $BrCH_2CH_2OH$ desorption. The inset shows the relative yield of $BrCH_2CH_2OH$ as a function of the exposure.

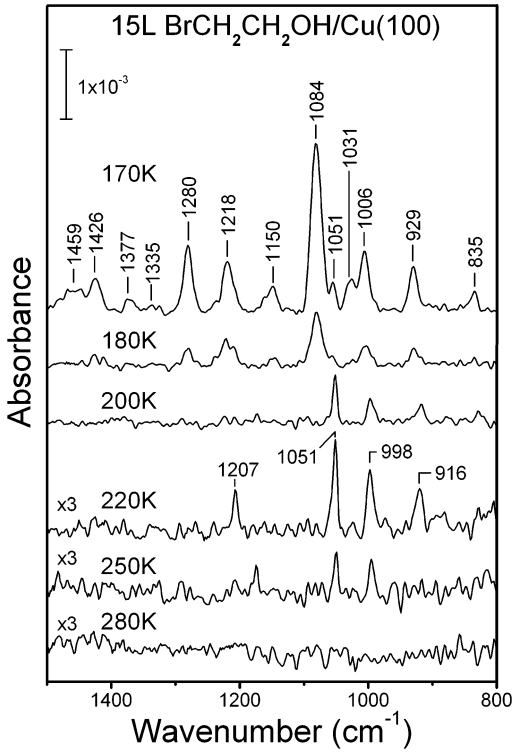

Figure 3. Reflection−absorption infrared spectra taken after exposing 15 L of $BrCH_2CH_2OH$ to Cu(100) at 115 K and flashing the surface to the temperatures indicated.

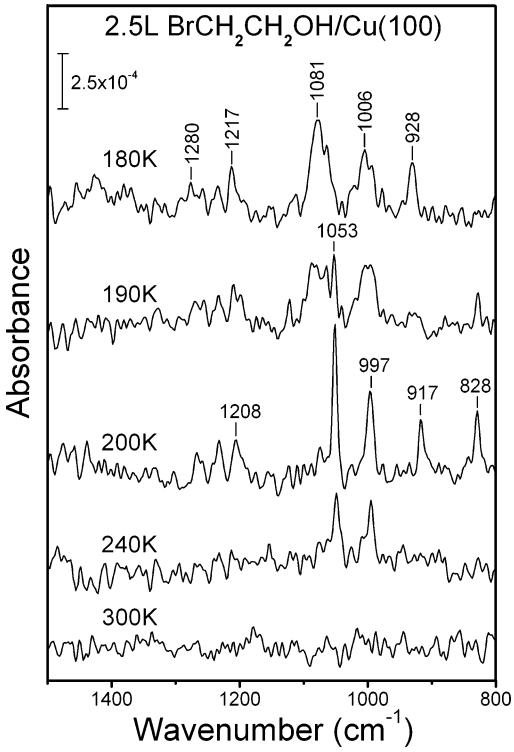

Figure 4. Reflection−absorption infrared spectra taken after exposing 2.5 L of $BrCH_2CH_2OH$ to Cu(100) at 115 K and flashing the surface to the temperatures indicated.

TABLE 1: Comparison of $BrCH_2CH_2OH$ Infrared Frequencies (cm^{-1})

15 L of $BrCH_2CH_2OH$ Cu(100), 170 K	$BrCH_2CH_2OH$[a]		mode description[b]
	liquid	vapor	
835	791	812	$\rho(CH_2)$
929	927	917, 924	$\rho(CH_2)$
1006	1003	1003	υ(C−C)
1031	1024		υ(C−C)
1051	1049	1047	υ(C−O)
1084	1071	1083	υ(C−O)
1150		1157, 1189	δ_{ip}(O−H)
1218	1214	1211, 1214	$\tau(CH_2)$, g
1280	1279	1254−1269	$\omega(CH_2)$, t
1335	1343	1349, 1355	$\tau(CH_2)$, t
1377	1374	1375, 1382	$\omega(CH_2)$, g
1426, 1459	1455	1418, 1444	$\delta(CH_2)$

[a] From ref 10. [b] υ, stretching; ρ, rocking; ω, wagging; δ, bending; τ, twisting; ip, in plane; g, gauche; and t, trans.

intensity simultaneously without forming new bands. This is explained by partial $BrCH_2CH_2OH$ molecular desorption, as supported by the TPR/D results in Figure 1. Upon heating to 200 K, we no longer observed the $BrCH_2CH_2OH$ bands, but new bands appeared. Absorptions grew at 916, 998, 1051, and 1207 cm^{-1} at 220 K. These bands diminished in intensity between 220 and 250 K and disappeared after the surface was heated to 280 K. The changes in spectral features between 180 and 200 K suggest that $BrCH_2CH_2OH$ on Cu(100) dissociates, forming new surface species. Similar temperature-dependent spectral changes are observed for the spectra that were measured at 3, 4, and 6 L.

Infrared Absorptions near and below the Monolayer Coverages on Cu(100). Figure 4 shows the temperature-dependent infrared spectra of a Cu(100) surface after dosing 2.5 L of $BrCH_2CH_2OH$ at 115 K. In the 180 K spectrum, the major infrared bands appear at 928, 1006, 1081, 1217, and 1280 cm^{-1}. All of the bands belong to the adsorbed $BrCH_2CH_2OH$. Similar spectra were measured at 115 and 150 K. Upon heating to 190 K, we observed the occurrence of a chemical transformation, with the evidence of a decrease of $BrCH_2CH_2OH$ and the formation of a new band at 1053 cm^{-1}. In the 200 K spectrum, adsorbed $BrCH_2CH_2OH$ is no longer observed and an absorption feature completely different from that of $BrCH_2CH_2OH$ appears, with major infrared bands located at 828, 917, 997, 1053, and 1208 cm^{-1}. When heated to 240 K, the two strongest bands at 997 and 1053 cm^{-1} are still observed. No infrared bands are detected in the 300 K spectrum. The spectral changing behavior with temperature is similar to that of 15 L. Therefore, it is concluded that the same surface species is generated from $BrCH_2CH_2OH$ decomposition at these two exposures. These temperature-dependent changes continue down to a submonolayer coverage. Figure 5 shows the infrared spectra of 1.5 L of $BrCH_2CH_2OH$ on Cu(100) as a function of temperature. The TPR/D study results in Figure 1 show no $BrCH_2CH_2OH$ molecular desorption at this exposure. In the 115 K spectrum, although the S/N ratios are poor, the bands due to the adsorbed $BrCH_2CH_2OH$ can be seen at 923, 1001, and 1078 cm^{-1}. When the surface is heated to 200 K, the adsorbed $BrCH_2CH_2OH$ decomposes to form new bands at 998 and 1050 cm^{-1}. Temperature-dependent spectra for 1 L of $BrCH_2CH_2OH$ were also recorded several times; however, no infrared peaks were detected due to poor S/N ratios.

Infrared Absorptions at Multilayer Coverages of $BrCH_2CH_2OH$ on O/Cu(100). Figure 6 shows the temperature-dependent IR spectra of an oxygen-precovered Cu(100) surface after dosing 15 L of $BrCH_2CH_2OH$ at 115 K. In the 165 K spectrum, the infrared bands appear at 834, 931, 1007, 1027, 1053, 1082, 1157, 1218, 1280, 1372, 1426, and 1459 cm^{-1}, which are attributed to $BrCH_2CH_2OH$. When the surface is heated to 185 K, the amount of adsorbed $BrCH_2CH_2OH$ decreases, as evidenced by the reduction of its most intense band at 1082 cm^{-1}. As a contrast, the bands at 1003 and 1053 cm^{-1} become relatively strong, suggesting that new surface

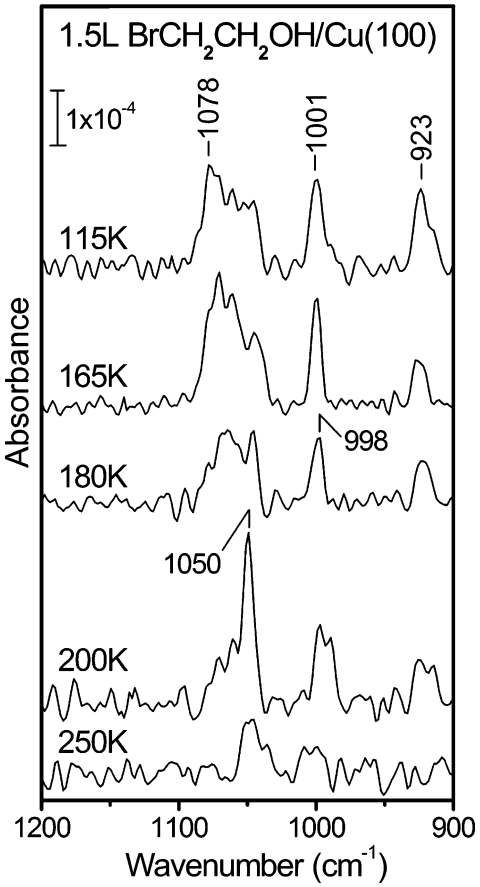

Figure 5. Reflection−absorption infrared spectra taken after exposing 1.5 L of $BrCH_2CH_2OH$ to Cu(100) at 115 K and flashing the surface to the temperatures indicated.

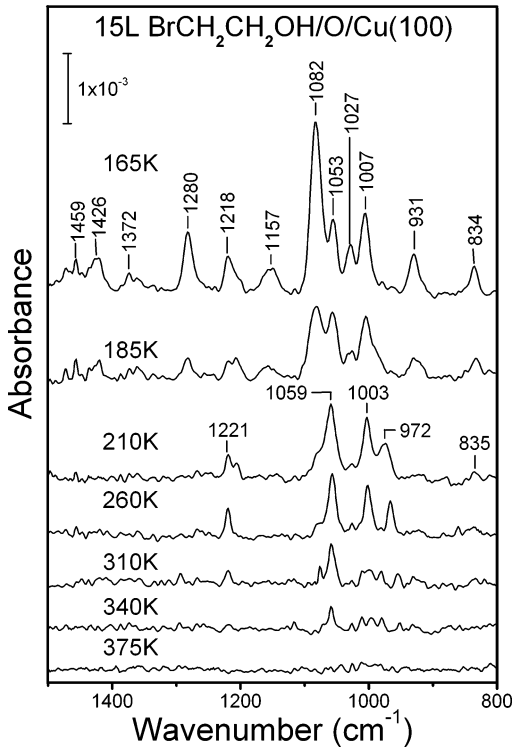

Figure 6. Reflection−absorption infrared spectra taken after exposing 15 L of $BrCH_2CH_2OH$ to oxygen-precovered Cu(100) at 115 K and flashing the surface to the temperatures indicated.

species are generated at this temperature. The $BrCH_2CH_2OH$ 1082 cm^{-1} band is hardly observable when heated to 210 K,

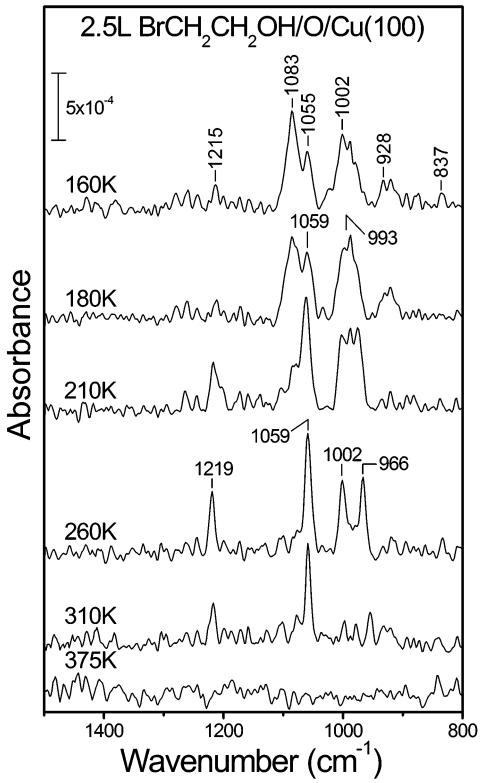

Figure 7. Reflection−absorption infrared spectra taken after exposing 2.5 L of $BrCH_2CH_2OH$ to oxygen-precovered Cu(100) at 115 K and flashing the surface to the temperatures indicated.

but a new set of bands appear at 835, 972, 1003, 1059, and 1221 cm^{-1} and remain about the same in the 260 K spectrum. These bands decrease in intensity when heated to 310 K. In the 375 K spectrum, no infrared bands are detected. Similar temperature-dependent spectral changes are observed for the spectra recorded at 6, 4, 2.5, and 1.5 L. Only the case for 2.5 L is shown below.

Infrared Absorptions near and below the Monolayer Coverages of $BrCH_2CH_2OH$ on O/Cu(100). Figure 7 shows the temperature-dependent IR spectra of an oxygen-precovered Cu(100) after dosing 2.5 L of $BrCH_2CH_2OH$ at 115 K. In the 160 K spectrum, the bands due to the adsorbed $BrCH_2CH_2OH$ appear at 837, 928, 1002, 1055, 1083, and 1215 cm^{-1}. The absorptions at 993 and 1059 cm^{-1} are slightly enhanced in the 180 K spectrum, revealing that a chemical transformation of $BrCH_2CH_2OH$ begins. Further heating to 210 K causes a significant loss of the adsorbed $BrCH_2CH_2OH$, as indicated by the diminished 1083 cm^{-1} band. The major absorptions appear at ∼990 and 1059 cm^{-1} in the 210 K spectrum. The former band is broad and likely due to an overlap of two or three bands. In the 260 K spectrum, the 1083 cm^{-1} $BrCH_2CH_2OH$ band disappears; there are four bands located at 966, 1002, 1059, and 1219 cm^{-1}. A similar set of bands is observed in the 260 K spectrum of 15 L. All of these bands decrease in intensity when heated to 310 K and disappear when further heated to 375 K.

Figure 8 shows the temperature-dependent spectra for 1.0 L of $BrCH_2CH_2OH$ on O/Cu(100). In the 115 K spectrum, the absorption bands appear at 832, 920, 1007, 1026, 1060, and 1083 cm^{-1}. The 1083 cm^{-1} band demonstrates the presence of $BrCH_2CH_2OH$ on O/Cu(100). However, the intensity ratios of 1007/1083 and 1060/1083 cm^{-1} are much larger than those for the similar bands observed in the 15 L, 115 K spectrum of Figure 6. This difference may result from the coverage-

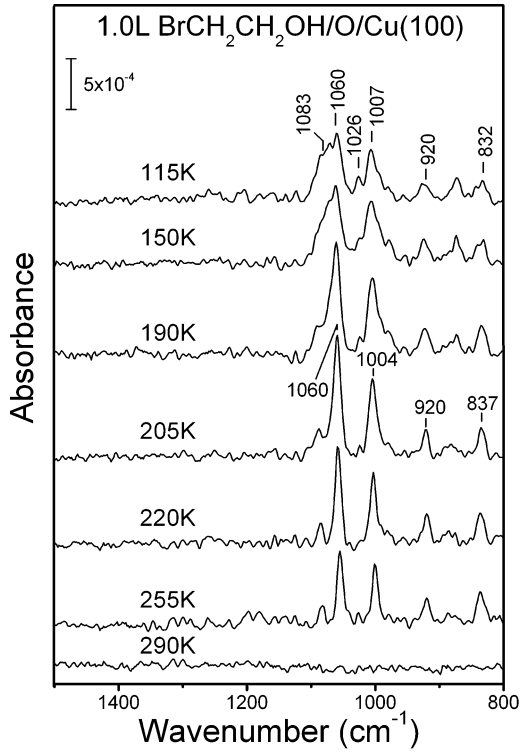

Figure 8. Reflection−absorption infrared spectra taken after exposing 1 L of $BrCH_2CH_2OH$ to oxygen-precovered Cu(100) at 115 K and flashing the surface to the temperatures indicated.

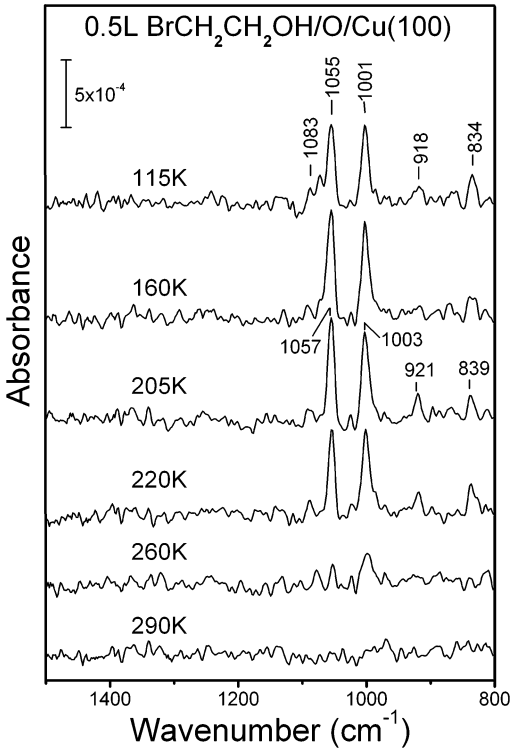

Figure 9. Reflection−absorption infrared spectra taken after exposing 0.5 L of $BrCH_2CH_2OH$ to oxygen-precovered Cu(100) at 115 K and flashing the surface to the temperatures indicated.

dependent $BrCH_2CH_2OH$ adsorption orientations and/or the dissociation of $BrCH_2CH_2OH$. The spectral feature does not change when heated to 150 K. Heating to 205 K enhances the absorptions at 837, 920, 1004, and 1060 cm^{-1} at the expense of the 1083 cm^{-1}, indicating $BrCH_2CH_2OH$ decomposition and new species formation. The spectral feature remains about the same when the surface is heated to 220 K. These four bands are no longer observed after heating to 290 K. Figure 9 shows the temperature-dependent spectra for 0.5 L of $BrCH_2CH_2OH$ on O/Cu(100). All of the spectra below 220 K are similar. There are four bands located at 839, 921, 1003, and 1057 cm^{-1} in the 205 K spectrum. These four bands have largely reduced intensities above 220 K, and disappear when heated to 290 K. The 115, 160, 205, and 220 K spectra in Figure 9 are similar to the 220 K spectrum in Figure 8 and cannot be attributed to absorbed $BrCH_2CH_2OH$. Therefore, it is concluded that $BrCH_2CH_2OH$ decomposes upon its adsorption on O/Cu(100) at 115 K at lower exposures.

Analysis of the Infrared Bands Detected from the $BrCH_2CH_2OH$ Decomposition on Cu(100) and O/Cu(100) Surfaces. Because the TPR/D studies of thermal reactions of $BrCH_2CH_2OH$ on Cu(100) and O/Cu(100), presented later, only show the desorption of ethylene and acetaldehyde (i.e., the carbon−carbon bond does not break in thermal decomposition of $BrCH_2CH_2OH$ on both surfaces), the following infrared analysis for Figures 3−9 is based on the adsorbed species with two carbon atoms. For a coverage from a multilayer (15 L) down to a submonolayer (1.5 L) on Cu(100), the infrared spectra of Figures 3−5 show that $BrCH_2CH_2OH$ is adsorbed molecularly at 115 K. In the case of 2.5 L exposure, the adsorbed $BrCH_2CH_2OH$ almost disappears by briefly heating to 200 K. The $BrCH_2CH_2OH$ consumption channels include desorption and dissociation. In Figure 4, a set of bands, not belonging to the absorbed $BrCH_2CH_2OH$, starts to appear as the surface is heated to a temperature of ∼190 K. They are located at 828, 917, 997, 1053, and 1208 cm^{-1}. When the surface is heated to a higher temperature of ∼280 K, this set of infrared bands disappears. For lower exposures of 0.5 and 1.0 L on O/Cu(100), a set of similar bands is observed. In the 1.0 L case, they appear at 837, 920, 1004, and 1060 cm^{-1} in the 205 K spectrum of Figure 7. These bands are hardly seen after briefly heating to a temperature of ∼290 K. The similarities in the infrared frequency and disappearance temperature suggest that the same surface species is generated on Cu(100) and O/Cu(100) from the decomposition of $BrCH_2CH_2OH$. It has been reported that the C−Br bond of propyl bromide breaks on Cu(111) between 160 and 220 K, and the O−H bond of FCH_2CH_2OH breaks on O/Cu(100) between 160 and 200 K.[11,12] Therefore, there are five surface intermediates (i.e., $BrCH_2CH_2O-$, $HOCH_2CH_2-$, $HOCH_2CH_2O-$, $-CH_2CH_2O-$, and $-OCH_2CH_2O-$) that are possibly generated from $BrCH_2CH_2OH$ decomposition on Cu(100) and O/Cu(100). Table 2 lists the band frequencies of the 2.5 L, 200 K spectrum of Figure 4 and the 1.0 L, 205 K spectrum of Figure 8. Those for $HOCH_2CH_2O-$ and $-CH_2CH_2O-$ on Ag(110) and Ag(111), generated by ICH_2CH_2OH decomposition, and $-OCH_2CH_2O-$ on O/Cu(100), generated by $HOCH_2CH_2OH$ decomposition, are also given for purposes of comparison.[13−15] Although $-OCH_2CH_2O-$ is a species likely to be formed as $BrCH_2CH_2OH$ dissociates on O/Cu(100), it is not generated, judging by the inconsistent frequencies listed in Table 2. In the last three columns of Table 2 for the observed frequencies and mode assignments of $HOCH_2CH_2-$ on Ag(111) and on Ag(110) from ICH_2CH_2OH decomposition, the C−O stretching vibrations absorb at 1070 and 1076 cm^{-1}, respectively, which are close to the value of 1073 cm^{-1} of ICH_2CH_2OH in matrix and to the value of 1068 cm^{-1} of ICH_2CH_2OH in a liquid state.[10] This means that the effect on the C−O stretching frequency is small as ICH_2CH_2OH dissociates by C−I breakage on the Ag surfaces to form $HOCH_2CH_2-$, in which the $HOCH_2$ moiety still remains intact. As a contrast, on Ag(110), the C−O

TABLE 2: Comparison of Infrared Frequencies (cm^{-1}) of $-CH_2CH_2O-$, $-OCH_2CH_2O-$, and $HOCH_2CH_2-$

$BrCH_2CH_2OH$[a]		$-CH_2CH_2O-$			$-OCH_2CH_2O-$		$HOCH_2CH_2-$		
Cu(100), 2.5 L, 200 K	O/Cu(100), 1.0 L, 205 K	Ag(111)[b]	Ag(110)[c]	mode[d]	O/Cu(100)[e]	mode	Ag(111)[b]	Ag(110)[c]	mode[d]
828	837	800	793	υ(C−C−O)			820	793	$\rho(CH_2)$
917	920	910		τ(C−C)	880	$\rho(CH_2) + \nu$(C−C)	910		$\rho(CH_2)$
997	1004	970	996	υ(C−O)			980	972	ν(C−C)
1053	1060	1060	1052	δ(C−C−O)	1090	ν(C−O)	1070	1076	υ(C−O)
							1170	1150, 1175	δ(C−OH)
1208			1218	$\tau(CH_2)$					
		1260	1278	$\omega(CH_2)$			1267	1255	$\omega(CH_2)$

[a] This work. [b] From ref 13. [c] From ref 14. [d] υ, stretching; τ, twisting; δ, bending; ω, wagging; and ρ, rocking. [e] From ref 15.

TABLE 3: Comparison of Experimental and Theoretical Infrared Frequencies (cm^{-1}) of $-CH_2CH_2O-$

$-CH_2CH_2O-$[a]	theoretical $-C^1H_2C^2H_2O-$[b]	approximate mode[c]
837	840	υ(C−C−O) + $\omega(C^1H_2)$ + $\rho(C^2H_2)$
920	890	τ(C−C) + $\tau(C^1H_2)$ + $\rho(C^2H_2)$
1004	1021	υ(C−O)
1060	1070	δ(C−C−O) + $\omega(C^1H_2)$
	1140	$\tau(C^1H_2)$ + $\tau(C^2H_2)$
	1167	$\omega(C^1H_2)$ + $\tau(C^2H_2)$

[a] $BrCH_2CH_2OH$ (1.0 L) at 205 K on O/Cu(100). [b] On Cu dimer. [c] υ, stretching; ρ, rocking; ω, wagging; δ, bending; and τ, twisting.

stretching frequency of CH_3CH_2O- is 24 cm^{-1} lower than that of $HOCH_2CH_2-$.[14,16] In our observed frequencies in the 2.5 L, 200 K spectrum of Cu(100) and the 1.0 L, 205 K spectrum of O/Cu(100), the C−O stretching band at ~1080 cm^{-1} is very small and hardly detectable, suggesting that the $HOCH_2$ moiety either is absent or has a tiny amount on the surfaces. Furthermore, in the thermal decomposition study of FCH_2CH_2OH on O/Cu(100), the O−H dissociates between 160 and 200 K;[12] therefore, the bands listed in the first two columns of Table 2, which are still observable at ~250 K in Figures 4 and 8, are not attributed to $HOCH_2CH_2-$. However, these band frequencies closely match the oxametallacycle ($-CH_2CH_2O-$) ones. In terms of the well-matched frequencies together with the known dissociation kinetics of C−Br and CO−H on Cu(100) and O/Cu(100), it is reasonable to believe that $-CH_2CH_2O-$ is generated as an intermediate during the $BrCH_2CH_2OH$ thermal decomposition on Cu(100) and O/Cu(100). In our recent study of the decomposition of 0.5 L of ICH_2CH_2OH on O/Cu(100), infrared bands at 981 and 1055 cm^{-1} with comparable intensities are detected in the spectra taken between 115 and 200 K.[17] These two bands are similar to the two strongest bands observed in the spectra of 115−220 K of Figure 8 for 0.5 L of $BrCH_2CH_2OH$ on O/Cu(100), suggesting the same species is generated from the decompositions of 0.5 L of $BrCH_2CH_2OH$ and ICH_2CH_2OH. The study of propyl iodide adsorption on Cu(100) has shown that the C−I bond dissociation temperature is below 120 K.[11] Therefore, the surface intermediate generated from the decompositions of 0.5 L of $BrCH_2CH_2OH$ and 0.5 L of ICH_2CH_2OH on O/Cu(100) is unlikely to be $BrCH_2CH_2O-$ or ICH_2CH_2O-.

Density functional theory calculations were employed to predict the infrared spectrum of an optimized structure of $-CH_2CH_2O-$ bonded to two copper atoms. Figure 10 shows the optimized Cu−CH_2CH_2O−Cu structure with physically realistic bond lengths and compares its theoretical infrared spectrum with the 205 K spectrum in Figure 8. No scaling factor was used for the predicted infrared frequencies. Due to the restriction of RAIRS to the dipole-scattering selection rules which affect the intensity of the bands observed in the RAIRS experiments, direct intensity comparison should not be emphasized. The experimental infrared bands of 1.0 L of 205 K

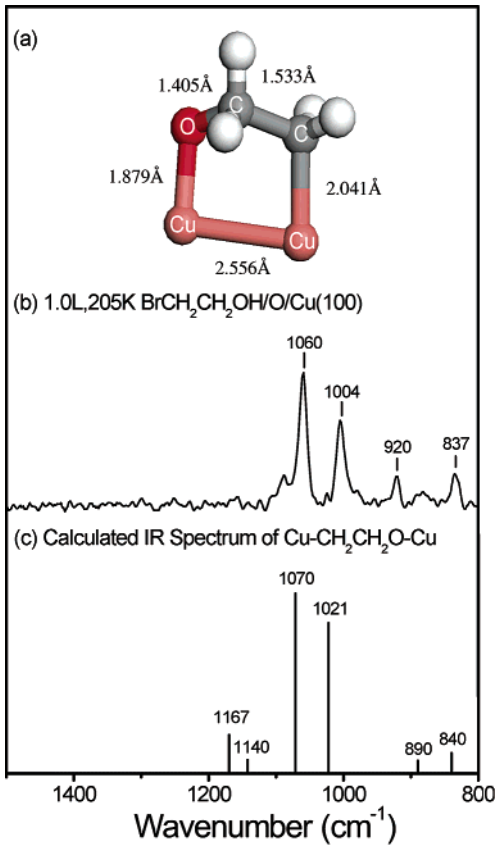

Figure 10. Optimized structure of $-CH_2CH_2O-$ bonded to a copper dimer (a); comparison between the calculated Cu−CH_2CH_2O−Cu spectrum and the 205 K spectrum of 1 L of $BrCH_2CH_2OH$ on oxygen-precovered Cu(100) (b and c).

$BrCH_2CH_2OH$ on O/Cu(100) and the theoretical ones of $-CH_2CH_2O-$ bonded to two Cu atoms are shown in Table 3. There is a good agreement, within 5% frequency differences, for the major modes of ν(C−C−O), τ(C−C), ν(C−O), and δ(C−C−O). The mode assignments in Table 3 are based on the animated vibrations of the corresponding bands. Only the main modes of functional groups are displayed in terms of the displacements of vibrating atoms. In the comparative studies of $-CH_2CH_2O-$ vibrational spectra obtained experimentally from ICH_2CH_2OH decomposition on Ag(110) and theoretically from DFT calculations using 2 and 12 silver atom clusters, a close correlation between the predicted frequencies for the clusters with different sizes has been shown, demonstrating that the computationally less-expensive silver dimer calculation is adequate for the description of the $-CH_2CH_2O-$ vibrational motions.[13] In addition, there is also a direct agreement between the calculated and observed spectra of $-CH_2CH_2O-$, with frequencies matching within 5%.[14]

TABLE 4: Comparison of Experimental and Theoretical Infrared Frequencies (cm^{-1}) of $BrCH_2CH_2O-$

	$BrC^1H_2C^2H_2O-$[a]			
$BrCH_2CH_2O-$[b]	2 Cu atoms	4 Cu atoms	9 Cu atoms	approximate mode[c]
	845 (6.7)	851 (1.0)	863 (21.6)	$\rho(C^1H_2) + \upsilon(C-C)$
966	910 (10.5)	920 (6.5)	926 (28.2)	$\omega(C^1H_2) + (C^2H_2)$
1002	1003 (7.3)	1017 (21.2)	1022 (7.1)	$\tau(C^1H_2) + (C^2H_2)$
1059	1085 (100)	1082 (100)	1037 (44.7)	$\upsilon(C-O)$
	1176 (20.6)	1178 (27.5)	1172 (1.8)	$\tau(C^1H_2) + (C^2H_2)$ for 1176, 1178 $\tau(C^1H_2) + (C^2H_2)$ for 1172
1219	1217 (0.4)	1240 (0.7)	1215 (4.1)	$\omega(C^1H_2) + (C^2H_2)$ for 1217, 1240 $\tau(C^1H_2) + \tau(C^2H_2)$ for 1215
	1265 (33.4)	1298 (92.8)	1293 (100)	$\omega(C^1H_2) + \tau(C^2H_2)$ for 1265, 1298 $\omega(C^1H_2) + \omega(C^2H_2)$ for 1293

[a] The numbers in parentheses are relative intensities. [b] $BrCH_2CH_2OH$ (2.5 L) at 260 K on O/Cu(100). [c] υ, stretching; ρ, rocking; ω, wagging; and τ, twisting.

In the studies of thermal decomposition of ICH_2CH_2OH on Ag(111) and Ag(110), it has been shown that the C−I bond dissociates first to form $HOCH_2CH_2-$, followed by further decomposition to form $-CH_2CH_2O-$.[13,14] Obviously, the kinetics for the C−I bond scission is faster than that of the O−H bond for adsorbed ICH_2CH_2OH on the Ag surfaces. In the present study of Cu(100), $-CH_2CH_2O-$ is generated from $BrCH_2CH_2OH$ decomposition at a temperature of ∼190 K for exposures from 1.5 to 15 L. Below 180 K, only infrared bands from the adsorbed $BrCH_2CH_2OH$ are observed. The direct transformation from the adsorbed $BrCH_2CH_2OH$ to $-CH_2CH_2O-$ shows the comparable dissociation kinetics of the C−Br and O−H of $BrCH_2CH_2OH$ on Cu(100). As stated in the Introduction, only a small fraction of a monolayer of C_2H_5OH can dissociate on Cu(100). In the present study, there is no molecular desorption at a $BrCH_2CH_2OH$ exposure ≤2 L (2.5 L is defined as about a monolayer coverage) on Cu(100); for example, the adsorbed $BrCH_2CH_2OH$ molecules decompose at elevated temperatures. This result shows the effect of the presence of the Br on the O−H bond dissociation. Furthermore, on O/Cu(100), the strong band at ∼1060 cm^{-1} already exists in the 115 K spectra of the 0.5 and 1.0 L exposures, suggesting that $-CH_2CH_2O-$ is produced at this low temperature. In the infrared spectra of higher $BrCH_2CH_2OH$ exposures (≥1.5 L) on O/Cu(100), the changes of spectral features with temperature are not the same as that for lower exposures (0.5 and 1.0 L). At higher exposures, as shown in Figures 6 and 7, a different spectral feature from that of the absorbed $BrCH_2CH_2OH$ at 115 K is observed at a temperature of ∼180 K, including an enhanced absorption at ∼1060 cm^{-1} and a broadened absorption at ∼990 cm^{-1}, which is accompanied by a decrease in the intensity of the adsorbed $BrCH_2CH_2OH$. On heating to a temperature of 260 K in the 2.5 L case (Figure 7), we noticed that the infrared bands appear at 966, 1002, 1059, and 1219 cm^{-1}. Similar bands are observed in the 260 K spectrum of 15 L of $BrCH_2CH_2OH$ (Figure 6). In the case of 1.0 L exposure on O/Cu(100), it is established that $-CH_2CH_2O-$, with major bands at 837, 920, 1004, and 1060 cm^{-1}, is generated from $BrCH_2CH_2OH$ decomposition. The presence of the strong 966 cm^{-1} band in the 260 K spectra of Figures 6 and 7 suggests that a new species, different from $-CH_2CH_2O-$, is generated at higher exposures. A contribution of $-CH_2CH_2O-$ to the 1002 and 1059 cm^{-1} bands in the 260 K spectrum of 2.5 L on O/Cu(100) cannot be ruled out since the two most intense bands of $-CH_2CH_2O-$ appear at similar frequencies. However, if the $-CH_2CH_2O-$ is present, the quantity may not be large, as indicated by the very small or undetected absorptions at ∼830 and 920 cm^{-1}. Furthermore, since the 880 and 1090 cm^{-1} bands are not observed, $-OCH_2CH_2O-$ is not considered to be generated at higher $BrCH_2CH_2OH$ exposures on O/Cu(100). $HOCH_2CH_2-$ and $BrCH_2CH_2O-$ are two possible species that are responsible for the set of bands at 966, 1002, 1059, and 1219 cm^{-1}, but $HOCH_2CH_2-$ can be ruled out by examining the C−O stretching frequencies and the suggested O−H dissociation temperatures of FCH_2CH_2OH and $ClCH_2CH_2OH$ on O/Cu(100).[12,17] The C−O stretching frequency of $HOCH_2CH_2-$ on Cu(100) is expected to be close to that of $BrCH_2CH_2OH$ (i.e., at ∼1080 cm^{-1}), like the case of ICH_2CH_2OH on the Ag surfaces as shown in the last three columns of Table 2. However, an absorption band near 1080 cm^{-1} is hardly detectable in the 260 K spectrum of 2.5 L of $BrCH_2CH_2OH$ on O/Cu(100). In addition, the O−H bond of $BrCH_2CH_2OH$ on O/Cu(100) cannot remain intact at 260 K, as suggested by the O−H dissociation temperature between 160 and 220 K for $ClCH_2CH_2OH$[17] and FCH_2CH_2OH[12] on O/Cu(100). Although $BrCH_2CH_2O-$ is not found in the lower coverages (0.5 and 1 L), it can exist as a stable intermediate on O/Cu(100) at higher coverages because the number of surface-empty sites for its further dissociation is limited under crowded environments. In this case, $BrCH_2CH_2O-$ may decompose at temperatures higher than the lower-exposure cases.

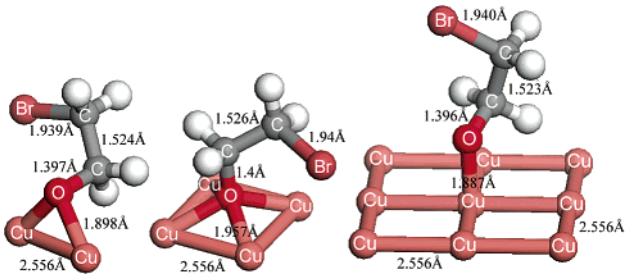

Figure 11. Optimized structures of $BrCH_2CH_2O-$ bonded to three different copper clusters.

Density functional theory calculations were employed to predict the infrared spectra for three optimized structures of $BrCH_2CH_2O-$ bonded to clusters of Cu with 2, 4, and 9 atoms (as shown in Figure 11) to mimic a surface adsorption at a bridging, a 4-fold hollow, and a top site, respectively, for adsorbed $BrCH_2CH_2O-$ on Cu(100). Table 4 compares the experimental and theoretical infrared frequencies. Although the bonding sites for the adsorbed $BrCH_2CH_2O-$ are still unknown, the experimental frequencies agree with the three theoretical ones, with a maximum discrepancy of ∼6%, showing that the vibrational motions of the organic adsorbate, $BrCH_2CH_2O-$, are not significantly affected by the bonding sites on the copper clusters. The C−O stretching mode of $BrCH_2CH_2O-$ is relatively more sensitive to the bonding sites than the other modes because the O atom is directly bonded to the copper clusters.

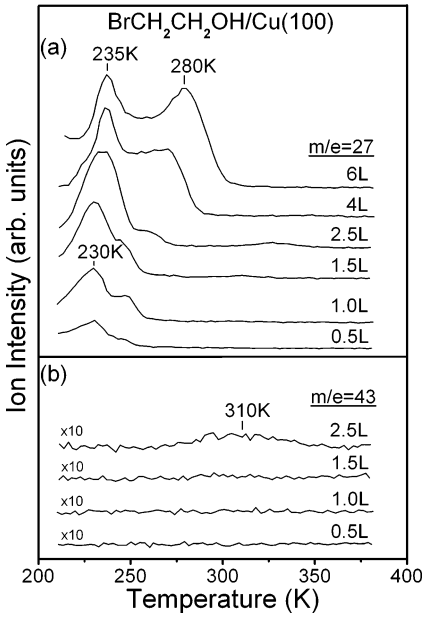

Figure 12. Temperature-programmed reaction/desorption spectra of a Cu(100) surface after dosing the indicated $BrCH_2CH_2OH$ exposures at 115 K, collected for the ions of $C_2H_3^+$ (a) and $C_2H_3O^+$ (b), representative of C_2H_4 and CH_3CHO desorption, respectively.

Surface oxametallacycles ($-C(R)(R')-C(R)(R')O-$, R = R′ = H or alkyl groups) have often been invoked as crucial intermediates for explaining the reactions of oxygenated hydrocarbons and the oxidation of alkenes on metal surfaces, such as ethylene oxide on Ag(111), Pd(110), Pd(111), and Ru(111),[18−21] ethanol on Rh(111),[22] 2-methylpropanol on Rh(111),[23] *tert*-butyl alcohol on Ag(110) and O/Rh(111),[24,25] propene and isobutene on O/Rh(111),[26,27] and ICH_2CH_2OH on Ag(111), Ag(110), and Ni(100).[13,14,28,29] Among these investigations, only the cases of ethylene oxide and ICH_2CH_2OH on the Ag surfaces provide convincing spectroscopic support for the formation of $-CH_2CH_2O-$.[13,14,22,28] In homogeneous media, metallaoxetanes, analogues of surface oxametallacycles, have been proposed as the reaction intermediates in alkene oxidation promoted by the oxotransition metal complexes, metal-assisted deoxygenation of epoxides, and so forth.[30,31] Examples of stable metallaoxetanes can be found in Ir and Zr complexes.[32−34]

TPR/D Studies of $BrCH_2CH_2OH$ on Cu(100). The results of infrared studies of $BrCH_2CH_2OH$ on Cu(100) have established that the $BrCH_2CH_2OH$ starts to decompose at a temperature of ∼190 K to form $-CH_2CH_2O-$ for the exposures of 1.5, 2, 2.5, 3, 4, 6, and 15 L that were investigated. $-CH_2CH_2O-$ on Cu(100) decomposes at a temperature higher than 200 K and is no longer observed above 280 K. Figure 12 shows the TPR/D spectra of the C_2H_4 desorption, represented by m/e = 27 amu, and that of the CH_3CHO desorption, represented by m/e = 43 amu, for the indicated $BrCH_2CH_2OH$ exposures on Cu(100). Identification of C_2H_4 is based on the fragmentation pattern of the major ions of 25, 26, and 27 amu, and that of CH_3CHO is based on the fragmentation pattern of the major ions of 15, 29, and 43 amu. In Figure 12a, maximum desorption rates occur at ∼230 K for an exposure ≤2.5 L. For 4 and 6 L, there are two comparable desorption peaks centered at 235 and 280 K. In our infrared studies of Cu(100), the spectral S/N ratios are poor below 1.5 L of $BrCH_2CH_2OH$, not allowing for the intermediate detection; however, it can be concluded that $-CH_2CH_2O-$ is generated from $BrCH_2CH_2OH$ decomposition on Cu(100) at lower coverages (<1.5 L) as well, based on the similar C_2H_4 desorption feature between 0.5 and 2.5 L. In Figure 12b, the CH_3CHO signals are very small and hardly detectable.

TPR/D Studies of $BrCH_2CH_2OH$ on O/Cu(100). The results of the infrared studies of $BrCH_2CH_2OH$ on O/Cu(100), as shown in Figures 6−9, have established that $-CH_2CH_2O-$ is generated at an exposure <1.5 L and that $BrCH_2CH_2O-$ is generated at an exposure ≥1.5 L, although the possibility for the presence of $-CH_2CH_2O-$ cannot be ruled out at higher exposures. Figure 13 shows the TPR/D spectra of C_2H_4 and CH_3CHO desorptions, represented by m/e = 27 and 43 amu, respectively, for the indicated exposures of $BrCH_2CH_2OH$ on O/Cu(100). For the 0.5 and 1.0 L traces in Figure 13a, C_2H_4 desorbs with a maximum rate at 290 K. On the basis of IR studies, this desorption feature is due to $-CH_2CH_2O-$ decomposition on O/Cu(100). The main C_2H_4 evolution temperature from $-CH_2CH_2O-$ decomposition on O/Cu(100) is about 60 K higher than that on Cu(100) at 0.5 and 1.0 L. For an exposure ≥1.5 L, C_2H_4 shows desorption behavior different from that of 0.5 and 1.0 L. This result is consistent with the exposure-dependent infrared absorptions. At higher exposures, C_2H_4 desorption is extended toward higher temperatures, up to ∼400 K, with two broad peaks at ∼315 and 370 K. The infrared results suggest that $BrCH_2CH_2O-$ is the main surface intermediate for the desorption features. In Figure 13b, for CH_3CHO desorption,

SCHEME 1

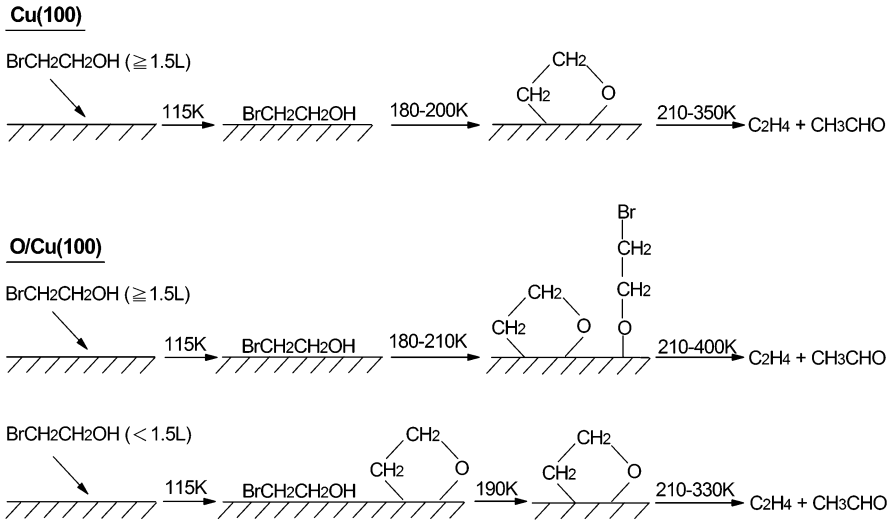

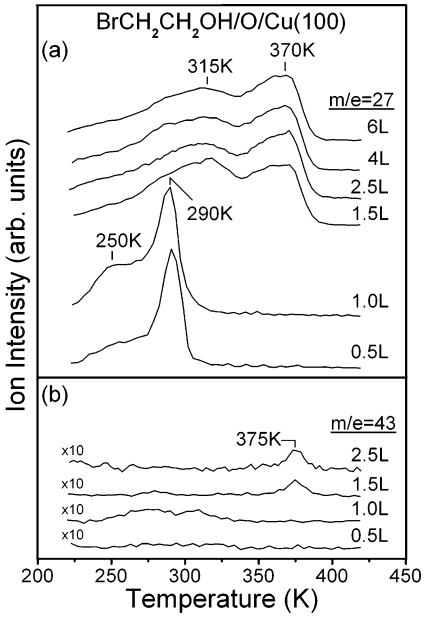

Figure 13. Temperature-programmed reaction/desorption spectra of an oxygen-precovered Cu(100) surface after dosing the indicated $BrCH_2CH_2OH$ exposures at 115 K, collected for the ions of $C_2H_3^+$ (a) and $C_2H_3O^+$ (b), representative of C_2H_4 and CH_3CHO desorption, respectively.

a tiny, broad peak appears at ~290 K at 1.0 L $BrCH_2CH_2OH$. At a $BrCH_2CH_2OH$ exposure ≥1.5 L, CH_3CHO mainly desorbs at 375 K.

$-CH_2CH_2O-$ has often been suggested as the intermediate in silver-catalyzed ethylene epoxidation. However, on Ag(110) and Ag(111), the decomposition of $-CH_2CH_2O-$ generated from ICH_2CH_2OH, forming ethylene oxide, is not observed. Interestingly, $-CH_2CH_2O-$, generated from the decomposition of ethylene oxide, re-forms as ethylene oxide on Ag(111) at 300 K.[18] On Ag(110), γ-butyrolactone, acetaldehyde, ethanol, and ethylene are the reaction products of $-CH_2CH_2O-$.[14] Acetaldehyde is formed from $-CH_2CH_2O-$ decomposition on Ag(111) at a temperature >260 K.[13,28] Furthermore, $BrCH_2CH_2OH$ reactions on Ru(111) have been studied. Decomposition of $BrCH_2CH_2OH$ on Ru(111) releases CH_4 at 252 K via a reaction pathway analogous to the pinacol rearrangement to acetaldehyde.[35]

Conclusions

The combined results of the RAIRS and TPR/D studies show that $BrCH_2CH_2OH$ on Cu(100), from the exposures of 1.5−15 L that were investigated, decomposes to form $-CH_2CH_2O-$ at a temperature near 190 K. The oxametallacycle species decomposes to form C_2H_4 between 210 and 310 K. Precovered oxygen atoms play important roles in the $BrCH_2CH_2OH$ dissociation kinetics and surface species formations. For lower exposures of 0.5 and 1.0 L of $BrCH_2CH_2OH$ on O/Cu(100), $-CH_2CH_2O-$ is generated at a 115 K dosing temperature. At higher $BrCH_2CH_2OH$ exposures (≥1.5 L), $BrCH_2CH_2O-$ is the main species generated at a temperature of ~200 K. C_2H_4 and CH_3CHO desorption behaviors in the TPR/D studies of $BrCH_2CH_2OH$ on O/Cu(100) respond to the exposure-dependent surface intermediate formation. C_2H_4 and CH_3CHO desorb between 210 and 310 K at 0.5 and 1.0 L. However, the desorption is extended up to ~400 K at higher exposures. Scheme 1 shows the reaction pathways of $BrCH_2CH_2OH$ on Cu(100) and O/Cu(100). In addition, density functional theory calculations support the identification of the surface $-CH_2CH_2O-$ and $BrCH_2CH_2O-$ intermediates.

Acknowledgment. The work was supported by the National Center for High-Performance Computing and by the National Science Council of the Republic of China (NSC 92-2113-M-006-016).

References and Notes

(1) Lin, J.-L.; Teplyakov, A. V.; Bent, B. E. *J. Phys. Chem.* **1996**, *100*, 10721.
(2) Wachs, I. E.; Madix, R. J. *Appl. Surf. Sci.* **1978**, *1*, 303.
(3) Dai, Q.; Gellman, A. J. *J. Am. Chem. Soc.* **1993**, *115*, 714.
(4) Sexton, B. A. *Surf. Sci.* **1979**, *88*, 299.
(5) Camplin, J. P.; McCash, E. M. *Surf. Sci.* **1996**, *360*, 229.
(6) Wuttig, M.; Franchy, R.; Ibach, H. *Surf. Sci.* **1989**, *213*, 103.
(7) Rappe, A. K.; Casewit, C. J.; Colwell, K. S.; Goddard, W. A., III; Skiff, W. M. *J. Am. Chem. Soc.* **1992**, *114*, 10024.
(8) Delley, B. *J. Chem. Phys.* **2000**, *113*, 7756.
(9) *Density Functional Methods in Chemistry*; Labanowski, J. K., Andzelm, J. W., Eds.; Springer-Verlag: New York, 1991.
(10) Wyn-Jones, E.; Orgille-Thomas, W. J. *J. Mol. Struct.* **1967**−**1968**, *1*, 79.
(11) Lin, J.-L.; Bent, B. E. *J. Phys. Chem.* **1992**, *96*, 8529.
(12) Chen, C.-Y.; Chang, P.-T.; Kuo, K.-H.; Shin, J.-J.; Lin, J.-L. *J. Phys. Chem. B* **2003**, *107*, 10488.
(13) Linic, S.; Medlin, J. M.; Barteau, M. A. *Langmuir* **2002**, *18*, 5197.
(14) Jones, G. S.; Mavrikakis, M.; Barteau, M. A.; Vohs, J. M. *J. Am. Chem. Soc.* **1998**, *120*, 3196.
(15) Bryden, T. R.; Garrett, S. J. *J. Phys. Chem. B* **2001**, *105*, 9280.
(16) Dai, Q.; Gellman, A. *Surf. Sci.* **1991**, *257*, 103.
(17) Chang, P.-T.; Kuo, K.-H.; Shin, J.-J.; Chen, C.-Y.; Lin, J.-L. *Surf. Sci.*, in press.
(18) Linic, S.; Barteau, M. A. *J. Am. Chem. Soc.* **2002**, *124*, 310.
(19) Shekhar, R.; Barteau, M. A. *Surf. Sci.* **1996**, *348*, 55.
(20) Lambert, R. M.; Ormerod, R. M.; Tysoe, W. T. *Langmuir* **1994**, *10*, 730.
(21) Brown, N. F.; Barteau, M. A. *Surf. Sci.* **1993**, *298*, 6.
(22) Barteau, M. A.; Houtman, C. J. *J. Catal.* **1991**, *130*, 528.
(23) Barteau, M. A.; Brown, N. F. *J. Phys. Chem.* **1996**, *100*, 2269.
(24) Madix, R. J.; Brainard, R. L. *J. Am. Chem. Soc.* **1989**, *111*, 3826.
(25) Friend, C. M.; Xu, X. *Langmuir* **1992**, *8*, 1103.
(26) Friend, C. M.; Xu, X. *J. Am. Chem. Soc.* **1991**, *113*, 6779.
(27) Friend, C. M.; Xu, X. *J. Phys. Chem.* **1991**, *95*, 10753.
(28) Wu, G.; Stacchiola, D.; Kaltchev, M.; Tysoe, W. T. *Surf. Sci.* **2000**, *463*, 81.
(29) Zaera, F.; Zhao, B. Q. *J. Phys. Chem. B* **2003**, *107*, 9047.
(30) Jorgensen, K. A. *Chem. Rev.* **1989**, *89*, 431.
(31) Jorgensen, K. A.; Schiott, B. *Chem. Rev.* **1990**, *90*, 1483.
(32) Klein, D. P.; Hayes, J. C.; Bergman, R. G. *J. Am. Chem. Soc.* **1988**, *110*, 3704.
(33) Vaughan, G. A.; Hillhouse, G. H. *J. Am. Chem. Soc.* **1988**, *110*, 7215.
(34) Day, V. W.; Klemperer, W. G.; Lockledge, S. P.; Main, D. J. *J. Am. Chem. Soc.* **1990**, *112*, 2031.
(35) Brown, N. F.; Barteau, M. A. *J. Phys. Chem.* **1994**, *98*, 12737.